Geosciences **2014**, *4*, 31-49; doi:10.3390/geosciences4010031

OPEN ACCESS

geosciences

ISSN 2076-3263

www.mdpi.com/journal/geosciences

Article

Critical Factors Controlling Pd and Pt Potential in Porphyry Cu–Au Deposits: Evidence from the Balkan Peninsula

Demetrios G. Eliopoulos [1,*], Maria Economou-Eliopoulos [2] and Maria Zelyaskova-Panayiotova [3]

[1] Institute of Geology and Mineral Exploration (IGME), Sp. Loui 1, C Entrance, Olympic Village, GR-13677 Acharnai, Greece

[2] Depatment of Economic Geology and Geochemistry, Faculty of Geology and Geoenvironment, National and Kapodistrian University of Athens, Panepistimiopolis, GR-15784 Athens, Greece; E-Mail: econom@geol.uoa.gr

[3] Department of Geology, University of Sofia, Sofia 1504, Bulgaria; E-Mail: dobretenov@adiss-bg.com

* Author to whom correspondence should be addressed; E-Mail: eliopoulos@igme.gr; Tel.: +30-213-133-7313; Fax: +30-213-133-7440.

Received: 13 November 2013; in revised form: 28 February 2014 / Accepted: 28 February 2014 / Published: 12 March 2014

Abstract: Porphyry Cu–Au–Pd±Pt deposits are significant Au resources, but their Pd and Pt potential is still unknown. Elevated Pd, Pt (hundreds of ppb) and Au contents are associated with typical stockwork magnetite-bornite-chalcopyrite assemblages, at the central parts of certain porphyry deposits. Unexpected high grade Cu–(Pd+Pt) (up to 6 ppm) mineralization with high Pd/Pt ratios at the Elatsite porphyry deposit, which is found in a spatial association with the Chelopech epithermal deposit (Bulgaria) and the Skouries porphyry deposit, may have formed during late stages of an evolved hydrothermal system. Estimated Pd, Pt and Au potential for porphyry deposits is consistent with literature model calculations demonstrating the capacity of aqueous vapor and brine to scavenge sufficient quantities of Pt and Pd, and could contribute to the global platinum-group element (PGE) production. Critical requirements controlling potential of porphyry deposits may be from the metals contained in magma (metasomatized asthenospheric mantle wedge as indicated by significant Cr, Co, Ni and Re contents). The Cr content may be an indicator for the mantle input.

Keywords: porphyry; palladium; platinum; potential; transitional; Greece; Bulgaria

---

1. Introduction

Many important porphyry Cu–Au, Cu–Mo, Mo–W deposits are located around the Pacific rim, in Mediterranean and Carpathian regions of Europe, and in the Alpine-Himalayan system, extending from western Europe through Iran and the Himalaya to China and Malaysia (Figure 1). Porphyry Cu deposits typically have been formed along subduction-related convergent plate margins associated with island arcs and continental arcs or in extensional back-arc or post-collisional rift settings [1–11].

Alkaline or K-rich calc-alkaline porphyry deposits worldwide represent significant gold resources, owing to their large sizes. Moreover, during the last decades, elevated contents of palladium (Pd) and platinum (Pt) have been noted. These precious metals belong to the platinum-group elements (Os, Ir, Ru, Rh, Pd and Pt or platinum-group elements (PGEs)), which are the most valuable elements, of strategic importance, due to their growing use in advanced technologies (medicine, electronics) and automobile catalyst converters. Although they are traditionally associated with mafic-ultramafic complexes, significant Pd and Pt contents were described in certain alkaline porphyry deposits, such as the Cordillera of British Columbia (Copper Mountain, Galore Creek), Allard Stock, La Plana Mountains and Copper King Mine in USA [12,13], Skouries porphyry deposit, Greece [14,15], Elatsite, Bulgaria [16–19], Santo Tomas II in the Philippines [20,21] and elsewhere (Figure 1).

The research interest for many authors has been focused on the discovery of new PGE sources. Present study has focused on the characteristics of the Skouries (Greece) and Elatsite (Bulgaria) porphyry deposits. New and previously published geochemical data are combined with the current state of knowledge on the PGE solubility and partitioning of PGE which will lead to a better understanding of the controlling factors of the PGE mineralization and PGE potential in porphyry-Cu systems.

Figure 1. Location of porphyry Cu+Au+Pd±Pt deposits worldwide.

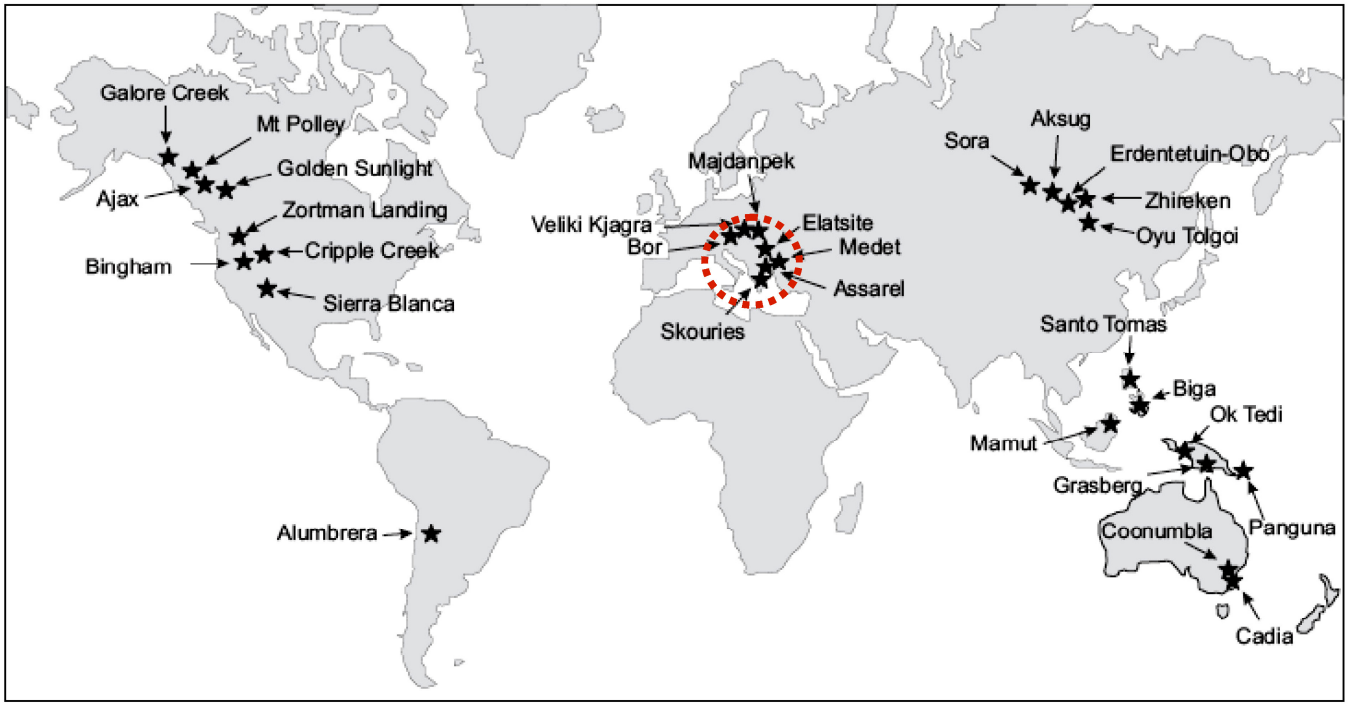

2. Analytical Methods

Polished sections were examined by reflected light combined with backscattered electron (BSE) images of the sections, obtained on a JEOL JSM 5600 (Tokyo, Japan) scanning electron microscope, at the University of Athens, Department of Geology and Geoenvironment.

Major- and minor-element compositions of precious metal-minerals were obtained using a JEOL JSM 5600 scanning electron microscope, equipped with an automated Oxford ISIS 300 (Oxfordshire, UK) energy dispersive analysis system, at the University of Athens, Department of Geology and Geoenvironment. Analytical conditions were 20 kV accelerating voltage, 0.5 nA beam current, <2 μm beam diameter and 50 s count times. The following X-ray lines were used: OsMα, PtMα, IrMβ, AuMα, AgLα, AsLα, FeKα, NiKα, CoKa, CuKα, CrKα, AlKα, TiKα, CaKα, SiKα, MnKα, MgKα, ClKα. Standards used were pure metals for the elements Os, Ir, Ru, Rh, Pt, Pd, Cu, Ni, Co and Cr, indium arsenide for As and pyrite for S and Fe.

Major and trace elements on mineralized porphyry samples were determined by inductively coupled plasma mass spectrometry (ICP-MS) analysis, at the Acme Laboratories Ltd., Vancouver, BC, Canada. Detection limits are 0.1 ppm for Ag, Cu, Pb, Ni, and Mo, 0.2 ppm for Co and 1 ppm for Zn and Cr. Platinum-group elements (PGE) were determined by ICP-MS analysis after pre-concentration using the nickel fire assay technique from large (30 g) samples, at the Acme Laboratories Ltd, Canada. This method allows for complete dissolution of samples. Detection limits are 10 ppb for Pt, 2 ppb for Pd and Au.

Oxygen isotopic and hydrogen compositions presented herein were determined on quartz veinlets containing Cu–Fe-minerals, magnetite and precious metal-minerals, at Geochron Laboratories. The hydrogen (δD) and oxygen ($\delta^{18}O$) data were normalized to the SMOW (Standard Mean Ocean Water) standard [22].

3. Characteristic Features and Results

3.1. Skouries Deposit (Greece)

The Skouries porphyry Cu–Au deposit, located at the Chalkidiki Peninsula, northern Greece, is hosted in the Vertiskos Formation of the Serbo-Macedonian massif (SMM) of Miocene age (18 Ma), which is younger than the intrusions of the Serbo-Macedonian massif (Figure 2).

The defined reserves in the porphyry Cu–Au deposit of Skouries are approximately 205 Mt at 0.5% Cu, and 0.53 ppm Au [23]. At least four monzonite porphyries have been described [24–27]. Two mineral assemblages of mineralization, occurring as veinlets/disseminations, can be distinguished: (a) magnetite-(reaching up to 10 vol %, average 6 vol %) bornite-chalcopyrite, linked to pervasive potassic and propylitic alteration, in the central parts of the deposit, and (b) chalcopyrite-pyrite, which dominates around the periphery of the deposit. Molybdenite occurs in small amounts, mainly at the marginal parts of the deposit that contains a minor quantity of chalcopyrite commonly in late pyrite-sericite-carbonate bearing veinlets [23–27]. Chalcopyrite, and to a lesser extent bornite are the main Cu-minerals.

Figure 2. Simplified geological map of the northern Chalkidiki Peninsula [23].

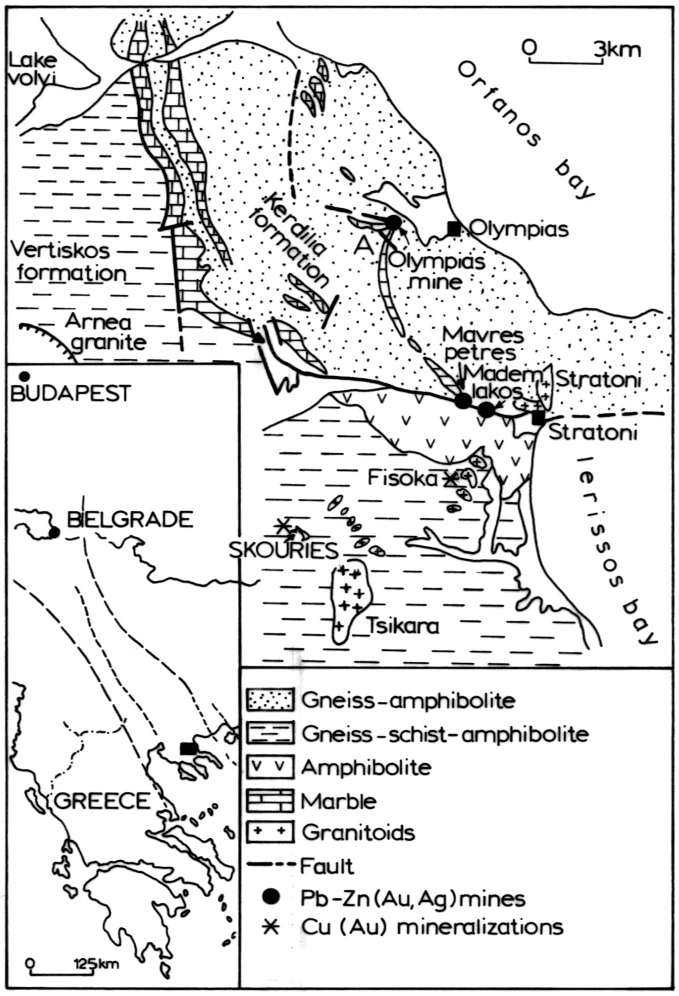

The most salient texture feature in the Skouries porphyry deposit is the intergrowth between merenskyite (Pd,Pt,Bi)Te_2, hessite (Ag_2Te), electrum and Cu-minerals (bornite and chalcopyrite) (Figure 3). Such an association of the palladium telluride, merenskyite, as the main PGE mineral in porphyry Cu–Au–Pd–Pt deposits, is considered to be of genetic significance and an important factor for the recovery of Pd and Pt as by-products. Relatively high Pd content in the major vein-type mineralization of Skouries has been documented by the analysis of a composite drill hole sample (~15 kg) showing 76 ppb Pd and 5000 ppm Cu [14,15].

Furthermore, mineralized material and highly mineralized portions (up to 2.5 wt % Cu) from deeper parts of the deposit (potassic, propylitic alteration zones) from drill holes covering the whole mineralized porphyry of Skouries (Figure 4) were analyzed for precious metals and trace elements (Table 1) in order to define their spatial distribution and probable interelement relationships.

A wide heterogeneity in the spatial variation of Cu, precious metal and trace element contents throughout the Skouries deposit is evident. A special attention was given to the chromium and nickel distribution, because they may provide evidence for the magma source and evolution of the mineralized system, due to their association with mafic-ultramafic rocks (parent magmas) and their compatible behavior [28,29]. There is a good positive correlation between Cr and Ni (R = 0.89, Table 1) at the Skouries porphyry.

Figure 3. Association of precious metal tellurides with chalcopyrite. Back-scattered electron (BSE) images showing (**a**) a close intergrowth of bornite (bn) with magnetite (mt), (**b**) chalcopyrite (Ccp) with galena (gn) and rutile (rt), (**c**) chalcopyrite with electrum (el) and hessite (hs), and (**d**) chalcopyrite with (Pd,Pt)-tellurides and electrum.

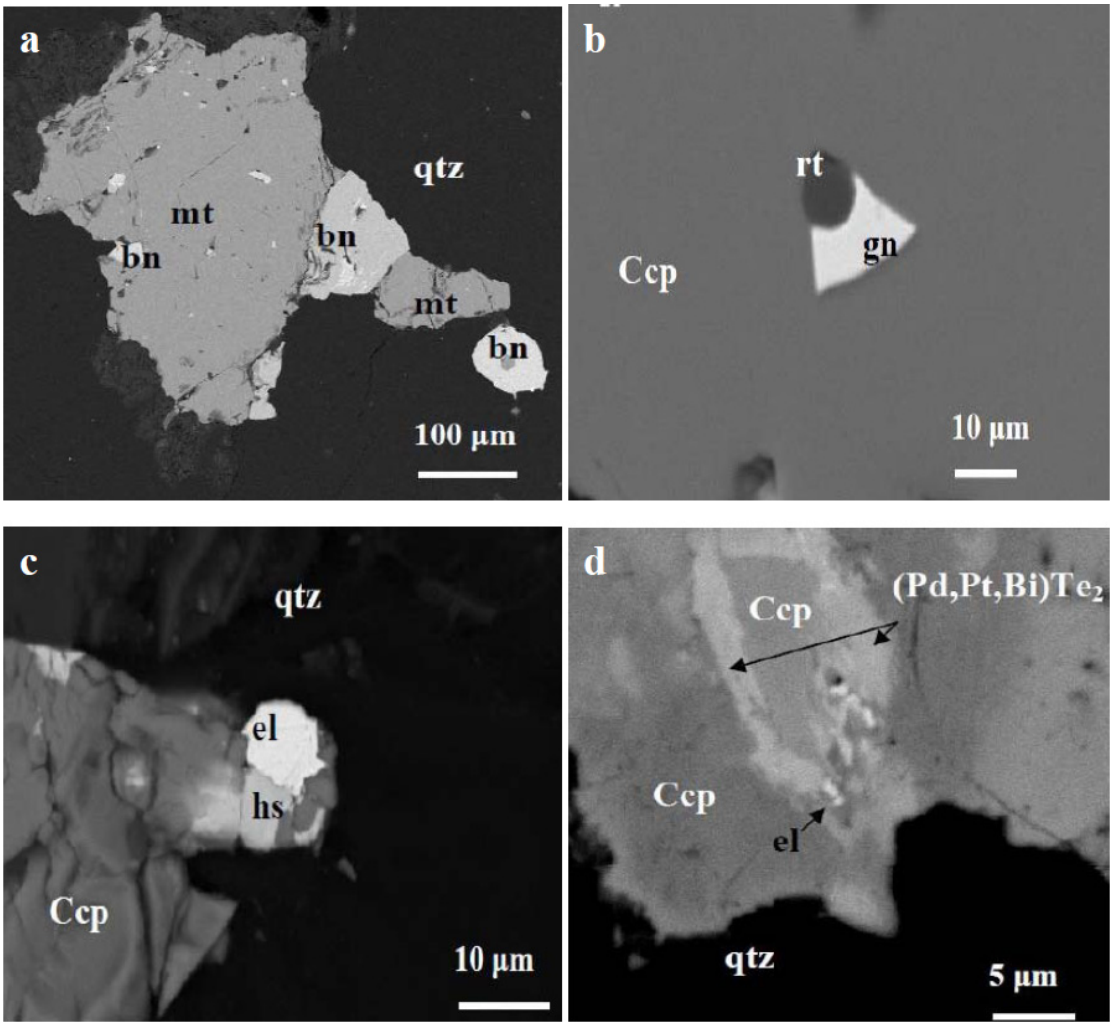

Table 1. Precious metal and selected trace element contents in the Skouries deposit. Symbols: Sk.PoF.C = flotation concentrate; *Sk.po. = composite drill-hole sample.

Sample	Depth m	Pd ppb	Pt ppb	Pd/Pt	Au ppb	Ag ppm	Cu wt %	Zn ppm	Pb ppm	Cr ppm	Ni ppm	Co ppm	Mo ppm
Sk.PoF.C.	--	2,400	40	60	22,000	110	21	17,000	110	20	90	76	20
*Sk.po.	--	76	<10	>7.6	910	3	0.5	150	25	30	38	25	2
sku400	surface	30	<10	>3.0	2,210	4.1	1.3	50	30	30	40	20	2
sku99	60	290	40	7.2	5,280	1.4	2.08	45	42	10	25	30	1
sku8	280	400	81	4.9	7,550	3.9	1.58	30	20	9	28	41	2
sku100	275	340	46	7.5	4,630	2.9	1.13	28	32	12	23	34	1
SOP 01	219	27	28	0.96	1,170	2.3	1.29	80	64	160	140	24	2
SOP 01	326	54	43	0.8	4,790	2.6	1.99	100	80	130	300	30	2
SOP 01	328	53	42	0.8	4,930	7	1.47	97	40	110	250	25	1

Table 1. *Cont.*

Sample	Depth m	Pd ppb	Pt ppb	Pd/Pt	Au ppb	Ag ppm	Cu wt %	Zn ppm	Pb ppm	Cr ppm	Ni ppm	Co ppm	Mo ppm
SOP 01	635	5	<10	>0.5	190	<0.2	0.06	38	21	50	42	26	2
SOP 01	636	3	<10	>0.3	50	<0.2	0.06	32	15	60	71	21	8
SOP 06	363	85	20	4.2	683	3.6	0.51	39	52	3	8	31	1
SOP 06	365	49	49	1	3,880	>10	1.27	80	60	10	210	24	2
SOP 06	525	29	22	0.76	549	1.3	0.68	110	34	260	310	62	1
SOP 06	527	6	<10	>0.6	120	<0.2	0.14	77	32	80	224	38	4
SOP 09	252	31	33	1.06	1,410	<0.2	1.1	73	30	8	50	35	3
SOP 18	142	42	64	1.52	3,850	2.4	1.52	75	84	4	50	22	2
SOP 18	178	16	26	1.62	532	0.7	0.8	67	110	6	30	30	11
SOP39	446	610	73	8.3	9,600	11.9	2.53	60	29	10	8	74	3
SOP 43	200	15	<10	>1.5	1,520	11.77	1.56	130	13	484	560	56	1
SOP 46	50	1	<10	>0.1	70	<0.2	0.14	94	50	125	127	29	240
SOP 76	170	2	<10	>0.2	590	0.6	0.71	180	12	690	504	41	100
SG-6	30	360	31	11.6	3,050	3.3	3.1	50	23	17	13	27	7
SG-6	110	28	10	2.8	850	0.5	0.39	66	71	6	17	62	2
SG-6	465	410	26	15.8	5,280	3.2	1.89	46	31	7	7	41	1
SG-6	494	420	150	2.8	12,900	3.4	2.84	60	21	17	10	43	<1
SK8	671	140	<10	>14	1,580	1.3	1.16	63	19	61	48	38	25

In addition, to constrain the origin of fluids trapped in quartz veins (which is unaltered in all alteration assemblages) stable isotope analyses of oxygen and hydrogen for quartz veins from various drill holes and depths performed. All samples were collected from depths of 60–525 m, covering the range of the recorded chromium contents (Table 1; Figure 4).

These data were used to calculate the isotopic composition of fluids in equilibrium with quartz, using as crystallization temperature minimum 350 °C and maximum 440 °C, based on the intergrowth of Cu–Fe sulphides and precious metal tellurides [30]. Isotopic trends of fluids, co-existing with quartz from various depths and drill holes in the Skouries porphyry Cu deposit are characterized by relatively high ($\delta^{18}O$ = 4.33‰–9.45‰) equilibrium fluid compositions (Table 2), which are comparable to those given in previous publications [26,31]. Furthermore, the analysis of D/H isotopes showed low δD (−110‰ to −73‰) values (Table 1).

Although any systematic variation of the isotopic data with depth is uncertain, it seems likely that the samples (group A) showing higher Cr contents (average = 290 ppm) correspond to lower calculated $\delta^{18}O$ values (average = 5.43) and those (group B) with lower Cr contents (average = 8.2 ppm Cr) correspond to higher $\delta^{18}O$ = 6.7‰ (Table 1; Figure 5). In addition, same samples with higher (Pd+Pt) contents (average = 274 ppb) and Pd/Pt ratios (average = 5.9) correspond to higher $\delta^{18}O$ values and lower Cr contents as well (Table 2).

Figure 4. Location of the studied drill holes, xenoliths and mineral intergrowths. (**a**) Location of drill holes in the Skouries porphyry [23], and (**b**) representative drill core sample, showing residues of assimilated dark green angular mafic fragments, and crosscutting relationships between successive quartz veins.

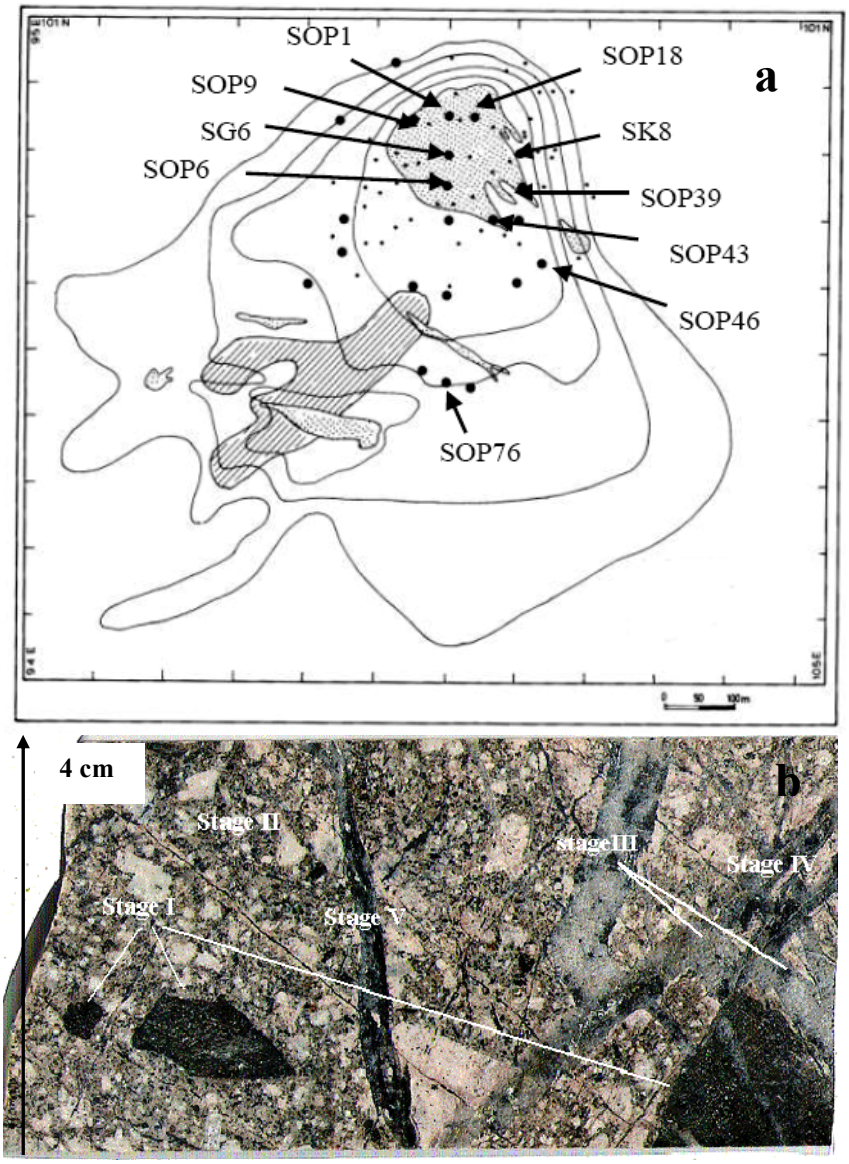

Table 2. Stable isotope analyses of quartz in mineralized veinlets from the Skouries porphyry deposit. Water compositions calculated using the min. (350 °C)/max. (440 °C) temperatures [30].

Samples	Depth	Cr	(Pd+Pt)	Pd/Pt	Mineral (measured)		Water (calculated)
	m	ppm	ppb		$\delta^{18}O_{(V\text{-}SMOW)}$ (‰)	$\delta D_{(V\text{-}SMOW)}$ (‰)	$\delta^{18}O_{(V\text{-}SMOW)}$ (‰)
A-group							
SOP06	525	260	51	0.76	9.7	−73	4.33–6.53
SOP43	200	480	24	1.6	9.6	−110	4.33–6.43
SOP01	326	130	55	0.96	9.7	−96	4.43–6.53
Average		290	43	1.1	9.7	−93	5.43

Table 2. *Cont.*

Samples	Depth m	Cr ppm	(Pd+Pt) ppb	Pd/Pt	Mineral (measured) $\delta^{18}O_{(V\text{-}SMOW)}$ (‰)	Mineral (measured) $\delta D_{(V\text{-}SMOW)}$ (‰)	Water (calculated) $\delta^{18}O_{(V\text{-}SMOW)}$ (‰)
B-group							
SOP09	479	8	64	1.1	12.6	−74	7.33–9.45
SOP18	178	4	42	1.6	11.3	−99	6.03–8.13
SG-6	465	7	436	16	9.6	−100	4.33–6.43
SOP06	367	10	98	1	9.6	−89	4.33–6.43
SOP39	446	10	679	8.3	10.9	−99	5.63–7.73
SKU99	60	10	328	7.2	11.5	−101	6.23–8.33
Average		8.2	274	5.9	10.9	−94	6.7

Figure 5. Relationship between calculated $\delta^{18}O$ values in quartz and Cr content. A plot of the calculated $\delta^{18}O$ values in quartz from mineralized quartz veinlets, in the range of maximum and minimum temperatures *versus* chromium content at the Skouries mineralized porphyry. The red squares represent average values for the groups A and B. Data from Tables 1 and 2.

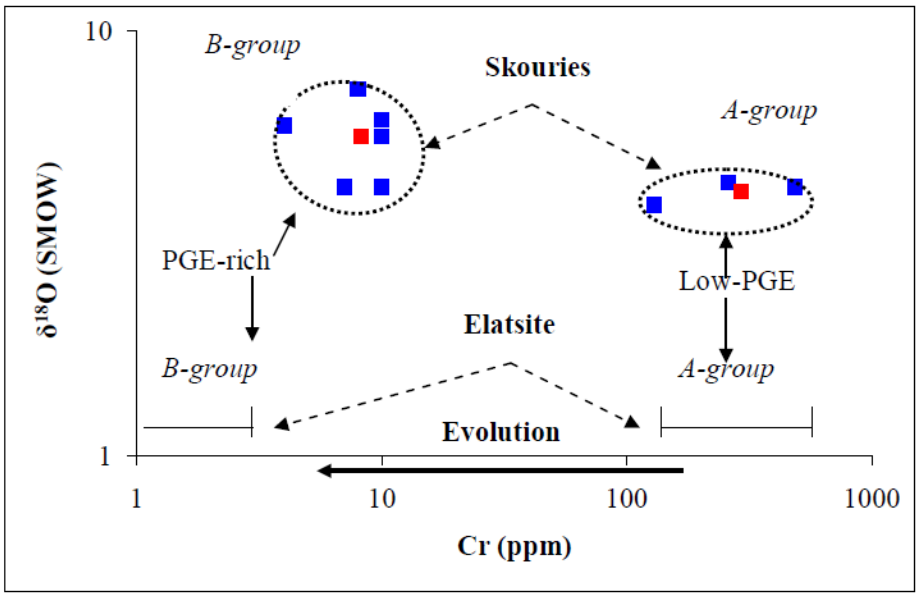

3.2. Fissoka Group

About 5 km east of Skouries is located the Fissoka porphyry (Figure 1), along the same structural trend, including several ore bodies within an area of about 1000 m × 600 m, and it is considered a prospect that may represent a separate deposit from that at Skouries. Diorite porphyry ages, 23.0 ± 1.2 (K–Ar on sericite) and 24.5 ± 1.2 Ma (K–Ar whole rock), at Fissoka suggest that the system is slightly older than Skouries [11]. Aeromagnetic data for the area suggests that the Skouries-Tsikara and the Fissoka areas are not connected in the shallow subsurface, and that only the supergene zone has been drilled to date. Several prospects are characterized by strong alteration, fissures with iron oxides and gossan, with anomalous copper in rock and soil samples [11]. Limited mineralogical data on the

eastern margin of the Fissoka porphyry Cu (OP-65 prospect) indicated disseminated mineralization consisting of pyrite with inclusion of gold, chalcopyrite, galena, sphalerite and arsenopyrite within the alteration zone, lower Pd and Cu content, Pd/Pt ratio and higher Au, Te, As, Pb and Zn content than at Skouries [15] suggest the prospect for further exploration.

4. Bulgaria

In Bulgaria, the Elatsite, Medet and Assarel, Petelovo and Tsar Assen porphyry-Cu deposits in the central Srednogorie metallogenetic zone (Figure 6) are related to multiphase monzonitic-monzodioritic stocks and dikes of Upper Cretaceous (92.3 ± 1.4 Ma) [32–34].

Figure 6. Simplified geological map showing the location of the main porphyry and epithermal deposits in the Srednogorie (Panagyurischte region) metallogenic zone. 1 = Precambrian gneiss, 2 = Paleozoic phyllite, 3 = Paleozoic granite, 4 = Paleozoic granodiorite, 5 = Triassic sediment, 6 = Cretaceous andesite, 7 = Cretaceous dacite, 8 = Cretaceous granite-granodiorite, 9 = Maastrichtian flysch, 10 = Tertiary conglomerate, 11 = Quaternary sediment, 12 = Fault, 13 = Au–Cu epithermal deposit, 14 = Cu porphyry deposit, 15 = Limit of the mineralized zones [33,34].

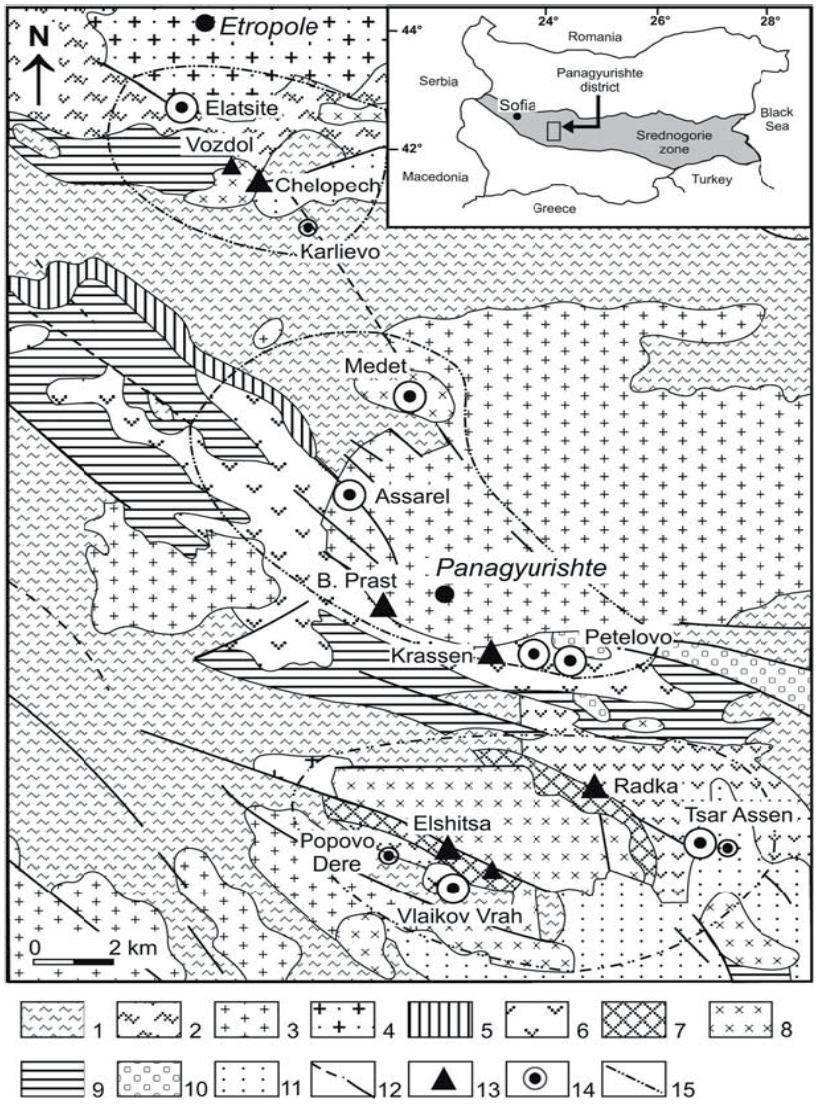

Elatsite

The Elatsite-Chelopech ore field can be divided into three sections: (a) the northern sector, the Elatsite porphyry Cu deposit is related to subvolcanic dikes and larger dike-like bodies intruding the basement rocks; (b) the central sector comprises the Chelopech volcano and associated subvolcanic intrusives, accompanied by the Chelopech Au–Cu massive high sulphidation deposit; and (c) the southern sector, a small intrusive body and several dikes intrude Precambrian metamorphic rocks along a system of radial-concentric faults [32–37].

Palladium, Pt and Au dominate in the mt–bn–cp assemblage, which is associated with potassic-propylitic alteration, while the pyrite–chalcopyrite assemblage is linked to phyllic and argillic alteration [18,19]. The average 890 ppb Au, 40 ppb Pd and 16 ppb Pt contents are higher in ore samples dominated by magnetite, bornite and chalcopyrite, compared to 460 ppb Au, 14 ppb Pd and 4 ppb Pt in samples consisting mainly of chalcopyrite and pyrite [16–19].

A salient feature is the unusually high precious metal content, recorded in high Cu-grade ores (magnetite-chalcopyrite-bornite) from the level 1310 South, which are similar to those analyzed by previous authors [18,19]; Table 3. In addition, the elevated Ag (up to 220 ppm), Bi (up to 290 ppm), Se (up to 800 ppm) contents, and the common occurrence of Au–Ag–Te–Se minerals in the magnetite-bornite-chalcopyrite ore assemblage [18,19] may be of genetic significance.

Plots of precious metals *versus* Cu (Figure 7) indicate that they define a broad positive trend between Cu and precious metal contents, and the Pd/Pt ratio, in contrast to the negative correlation between Pd and Cr contents. Given that there is a wide variation in the Cu-grade and the associated precious-metal ([18,19]; Table 3), the precious metal contents in the ore samples were normalized to 1% Cu, in order to obtain comparable data (Figure 7e). However, any clear correlation between Pd/Pt *vs.* Pd/Cu (Figure 7c) and Pd/Pt *vs.* (Pd+Pt) (Figure 7e), after re-calculation is uncertain.

Table 3. Precious metal, Cu and Cr contents in porphyry Cu deposits from Bulgaria. Symbols: py = pyrite; Ccp = chalcopyrite; bo = bornite; cc = chalcocite; mt = magnetite; cc = cuprite; Cu = native copper; n.a. = not available.

Deposit	Samples	Description	Pd ppb	Pt ppb	Pd/Pt	Au ppb	Cr ppm	Cu wt %
Elatsite	PC-E	mt–bo–cp	4,500	900	5	1,100	3	45.3
Elatsite	PC-31	mt–bo–cp	5,000	1,050	4.8	970	4	44.8
Elacite	PC-5	Ccp–py	4	20	0.2	100	10	12.8
Elacite	PC-6	Ccp–py	10	8	1.2	39	25	0.06
Elacite [18]	*n* = 6	Ccp–py	14	4.4	3.2	440	n.a.	0.64
Elacite [18]	*n* = 21	Ccp–py	130	26	5	4,630	n.a.	12.2
Elacite [18]	*n* = 8	mt–bo–Ccp	540	160	3.4	19,300	n.a.	20.3
Elacite [19]	*n* = 10	mt–bo–Ccp	26	14	1.9	670	430	0.8
Elacite [19]	EL-15	mt–bo–Ccp	3,440	320	11	1,820	<1	37
Elacite [19]	EL-26	mt–bo–Ccp	2,070	64	32	34,100	<1	37
Elacite [19]	EL-17	mt–bo–Ccp	980	350	2.8	7,800	<1	33.2
Elacite [19]	EL-18	mt–bo–Ccp	290	7	41	33,000	<1	49

Table 3. *Cont.*

Deposit	Samples	Description	Pd ppb	Pt ppb	Pd/Pt	Au ppb	Cr ppm	Cu wt %
Assarel	PC-2	Ccp–py	5	1.9	0.3	250	14	0.98
Assarel	PC-A1	Ccp–py	3	9	0.33	19,500	110	1.2
Assarel	PC-A2	Ccp–py	5	19	0.26	250	21	0.13
Assarel	PC-A3	Ccp–py	10	33	0.3	140	35	3.2
Medet	PC-4	Ccp–py	50	26	1.9	340	31	0.08
Medet	Mo-M	Ccp–py	33	47	0.7	35	6	0.17
Medet	PC-M2	Ccp–py	2	8	0.25	360	130	0.45
Medet	PC-M3	Ccp–py	50	26	1.8	340	31	2.15
Medet	PC-M4	Ccp–py	30	9	3.3	160	14	0.3
Tsar-Asen	PC-13	cp–Cu	49	51	0.96	95	100	0.93
Pechorovo	PC-17	Ccp–py	2	9	0.22	26	89	0.19
Pechorovo	PC-10	Ccp–py	2	8	0.25	20	11	0.18

Figure 7. Correlation between precious metals and Cu-grade. (**a**,**b**) Plots of the Au content and Pd/Pt ratios *versus* Cu content; (**c**) Pd/Pt ratio *vs.* Pd/Cu ratio; (**d**) Pd/Pt ratio *vs.* (Pd+Pt) content; (**e**) same Pd/Pt ratio *vs.* (Pd+Pt) after recalculation to 1 wt % Cu; and (**f**) Cr *vs.* Pd content, all for porphyry Cu–Au–Mo deposits. Data from Table 1 and 2, and [18,19,38,39].

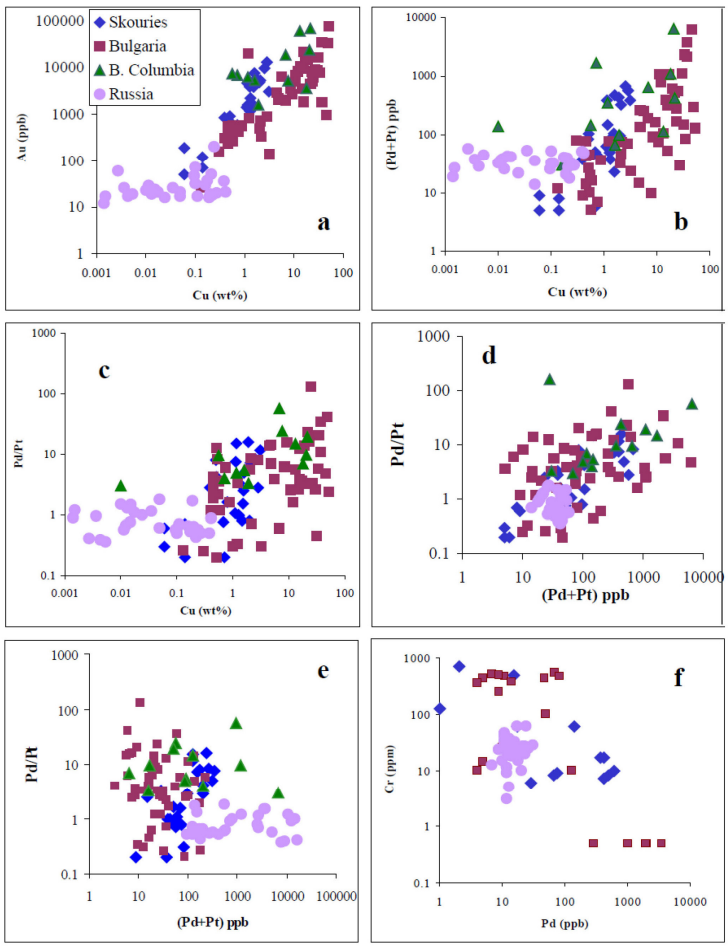

5. Discussion

Although more analytical data are required for the evaluation of the precious metal potential in porphyry deposits, examples from the Balkan Peninsula indicate that they may contribute significantly to the global PGE production. Using 206 Mt reserves [23] and average metal contents (0.5 wt % Cu, 75 ppb Pd and 17 ppb Pt [15], then the potential of the Skouries deposit is approximately 15 t Pd and 3.5 t Pt. In addition, using reserves and average Pd and Pt contents for the Elatsite deposit [33], the potential is about 13 t Pd and 3.47 t Pt. Such a precious metal potential is consistent with experimental data showing the ideal nature of porphyry-stage fluids for PGE scavenging, transport and deposition [40–46].

The metal potential in porphyry Cu+Au+Pd±Pt deposits may be related to the following factors:

5.1. Precious/Base Metal Endowment in Parent Magma

The enrichment in Cr, Co±Ni, recorded in the Skouries, Elatsite, Medet, Assarel and Tsar Assen porphyry deposits of the Balkan, having significant Pd and Pt contents, in contrast to the porphyry deposits of Russia and Mongolia with lower Pd–Pt content (less than 25 ppm Cr [39] supports the origin of their parent magma from an enriched mantle source [47–49]. Favorable tectonic settings include subduction of very young lithosphere or very slow or oblique convergence, flat subduction, and the cessation of subduction ([7,33,37,49–51]; Figure 8). The decreasing Pd, Pt contents, as well as in Re, from a few thousand ppm in porphyry Cu–Au deposits (Balkan Peninsula) to hundreds or tens of ppm in porphyry Cu–Mo type (Russia and Mongolia), and furthermore to less than tens of ppm Re in porphyry Mo–W (Lavrion, Greece) deposit [52–54] may be related to differences in their geotectonic environment.

The Re–Os system has been applied as both a geochronometer in molybdenite and as a tracer of the source of metals by direct determination of the source of Os in the ore minerals [55–63]. Elevated initial $^{187}Os/^{188}Os$ ratios (0.5–2.5) that are substantially more radiogenic than mantle indicate a contribution by a crust source (recycled in a metasomatized mantle, lower/upper continental crust) by inference other metals of porphyry Cu deposits and have been used to discern the influence of different reservoir [57,62]. On the basis of the initial $^{187}Os/^{188}Os$ ratios, a strong correspondence between copper tonnage and initial Os isotopic ratios (the larger deposits showed lower initial Os ratios than the smaller) has been established in Chilean porphyry deposits and American Southwest province (Bagdad, AZ, USA), suggesting a greater mantle component [63,64]. Also, elevated Os isotope compositions recorded in deposits of varying ages, have been interpreted to reflect recycling of discrete intracrustal domains with high $^{187}Os/^{188}Os$ ratios reflecting the process of crustal hybridization and homogenization [62]. Rhenium-osmium (Re–Os) ages and Re content data for molybdenites from the porphyry deposits in the Apuseni–Banat–Timok–Srednogorie (ABTS) magmatic metallogenic belt have shown high to extremely high Re and constrain the geochemical-metallogenic evolution of the belt in space and time [10]. The highest Re (thousands of ppm) and ^{187}Os (thousands of ppb) values were recorded in the Elatsite Cu–Au–Mo–(PGE) porphyry deposit, reflecting probably higher contribution from mantle of post-collisional mantle-derived magmas [49–51].

Therefore, Os isotope compositions provide new constraints on amounts of intra-crust recycling in young subduction-zone environments that reflect the magmatic history of the arc, as previously

suggested by Sr-, Nd- and Hf and Pb isotope data [35,65,66]. In addition, the initial $^{187}Os/^{188}Os$ values for sulphides from the Lavrion mine, suggest that ore-forming components were derived from mixed sources, one of which was a radiogenic crustal source, and the other, intrusive rocks that are less radiogenic [67].

Figure 8. Integrating magmatism and tectonics in the Srednogorie metallogenetic zone. Schematic diagram integrating magmatism in the Srednogorie metallogenetic zone with convergent margin tectonics (adapted from [50]).

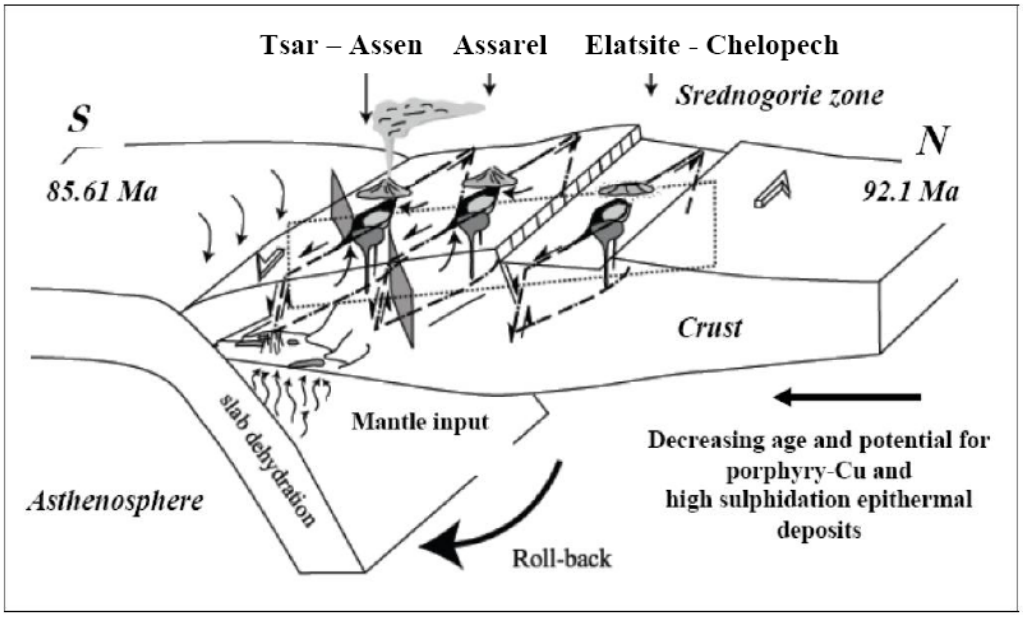

5.2. Physico/Chemical Conditions

Arc magmas with high potential to produce hydrothermal systems with ideal chemistry for transporting precious metals (origin of Au and Cu deposits) are characterized by fO_2 more than two log units above FMQ, where fO_2 is oxygen fugacity and FMQ is the fayalite-magnetite-quartz oxygen buffer [68,69]. It is consistent with the abundance of magnetite in all porphyry Cu–Au–Pd deposits of the Balkan Peninsula [14–19]. In contrast, "reduced" porphyry Cu–Au deposits, lacking primary hematite, magnetite, and sulphate minerals (anhydrite), contain abundant pyrrhotite, and are relatively Cu-poor, but Au-rich deposits [6].

Several experimental studies have shown that the low pH and high fO_2 nature of porphyry-stage fluids are ideal for PGE transport via chlorides, at relatively low-temperature [40–44]. Moreover, it has been demonstrated that sufficient quantities of Pt and Pd may be scavenged from the silicate magma by vapor and brine over the magmatic system [45,46].

5.3. Fractionation in the Mineralized System

Differences in the Pd/Pt ratios, ranging from 0.71 (up to 1.1) in the porphyry deposits of Russia and Mongolia, to 4.3 (up to 16) in Skouries, 10 (up to 130) in Elatsite and 13 (up to 57) in British Columbia, may reflect differences in their evolution systems. In addition, the extremely low Cr contents (<1 ppm) in high Cu–Pd–Pt-grade ores from Elatsite deposit (Table 3), and the increasing (Pd+Pt) content and

Pd/Pt rations with decreasing Cr content in the Skouries deposit (Table 2; Figure 4) are consistent with the compatible behaviour of Cr. There is a decoupling between precious metals and Cu in the plots Pd/Pt *vs.* (Pd+Pt) and Pd/Pt *vs.* Cu, after re-calculation of Pd and Pt values at the typical Cu-grade (~1 wt % Cu), due probably to the much higher values of the partition coefficient for Pd and Pt compared to that for Cu [48,70]. Nevertheless, the increasing (Pd+Pt) content with the increase of the Pd/Pt ratio (Figure 7), due to the more incompatible behavior of Pd than that of Pt [40–46] suggest an enrichment in Pt, Pd, Au, and Cu with fractionation. Thus, the magmatic component, as it is supporting by the $\delta^{18}O$ values in the liquid fluids carrying metals (Table 2), seems to be a driving force for the precious metal potential in evolved porphyry Cu deposits.

In addition, the elevated Au, Ag, Te, Bi, Se contents and the abundance of corresponding minerals, like tetrahedrite and tennantite, at the Elatsite deposit resemble geochemical and mineralogical characteristics of epithermal deposits, and have been interpreted as the latest stage of the porphyry system [18,33,34,38,49,51]. Hydrothermal veins in volcanic rocks, adjacent to Cu–Au porphyry mineralization, have been considered as the equivalent of transitional (post-porphyry, pre-epithermal) like in other porphyry Cu deposits [71]. The enrichment in Au, PGE, As, Sb, Hg, Bi, Te and base metals, has been attributed to the migration away from the source intrusion of mineralized fluids, resulting in the deposition of metals in the veins at a depth of up to several kilometers [71].

6. Conclusions

The compilation of new and previously published data on porphyry Cu–Au–Pd±Pt deposits, and differences within and between porphyry deposits, lead to the following conclusions:

- Critical requirements for a significant base/precious metal potential in porphyry Cu+Au+Pd±Pt deposits are considered to be the geotectonic environment, controlling the precious/base metal endowment in the parent magma, the oxidized nature of parent magmas, that facilitate the capacity for transporting sufficient Au and PGE, and the degree of evolution of the mineralized system.
- The elevated contents (hundreds of ppm) in Cr, Co, Ni and Re in porphyry Cu–Au–Pd±Pt deposits of the Balkan Peninsula, in contrast to the porphyry Cu–Mo deposits of Russia and Mongolia are attributed to a direct mantle input by metasomatized asthenospheric mantle wedge.
- The elevated values of the Pd/Pt ratios in porphyry deposits of the Balkan Peninsula, coupled with the extremely low Cr contents (<1 ppm) in high Cu–Pd–Pt-grade ores from Elatitse, and the negative correlation between Cr content and the Pd/Pt, $\delta^{18}O$ values, support their genesis from more evolved mineralized fluids.
- The Pd and Pt upgrade in massive Cu-ore at the Elatsite porphyry deposit may point to the possibility for their concentration in "transitional" porphyry deposits, during late stages of the evolution of the hydrothermal systems.
- The estimated Pd, Pt and Au potential for certain porphyry-Cu deposits are consistent with the capacity of aqueous vapor and brine to scavenge sufficient quantities of Pt, and Pd, and hence porphyry Cu–Au–Pd–Pt deposits may contribute significantly to global PGE production.

Acknowledgments

The University of Athens is greatly acknowledged for the financial support of this work (70/4/4535). Many thanks are expressed to the Mining Company TVX for providing representative samples from drill holes of the Skouries porphyry, two anonymous reviewers for their constructive criticism and suggestions on an earlier draft of the manuscript. Evagelos Michaelidis, University of Athens, is thanked for his assistance with the SEM/electron probe analyses.

Conflicts of Interest

The authors declare no conflict of interest.

References

1. Kirkam, R.V.; Sinclair, W.D. Porphyry Copper, Gold, Molybdenum, Tungsten, Tin, Silver. In *Geology of Canadian Mineral Deposit Types*; Eckstrand, O.R., Sinclair, W.D., Thorpe, R.I., Eds.; Geological Survey of Canada: Ottawa, ON, Canada, 1996; pp. 421–446.
2. Corbert, G.J.; Leach, T.M. *Southwest Pacific Rim Gold-Copper Systems*: *Structural*, *Alteration and Mineralization*; Society of Economic Geologists: Littleton, CO, USA, 1998.
3. Bookstrom, A.A.; Carten, R.B.; Shannon, J.R.; Smith, R.P. Origins of bimodal leucogranite-lamprophyre suites, climax and red mountain porphyry molybdenum systems, Colorado: Petrologic and strontium isotopic evidence. *Colo. Sch. Mines Q*. **1988**, *83*, 1–22.
4. Sillitoe, R.H. Gold-rich porphyry deposits; descriptive and genetic models and their role in exploration and discovery. *Rev. Econ. Geol.* **2000**, *13*, 315–345.
5. Sillitoe, R.H.; Hedenquist, J. Linkages between volcanotectonic setting, ore-fluid compositions and epithermal precious metal deposits. *Soc. Econ. Geol.* **2003**, *10*, 315–343.
6. Sillitoe, R.H. Porphyry copper systems. *Econ. Geol.* **2010**, *105*, 3–41.
7. Tosdal, R.M.; Richards, J.P. Magmatic and structural controls on the development of porphyry Cu±Mo±Au deposits. *Rev. Econ. Geol.* **2001**, *14*, 157–181.
8. Brooks, C.K.; Tegner, C.; Stein, H.; Thomassen, B. Re–Os and 40Ar/30Ar ages of porphyry molybdenum deposits in the east Greenland volcanic-rifted margin. *Econ. Geol.* **2004**, *99*, 1215–1222.
9. Richards, J.P. Tectono-magmatic precursors for porphyry Cu–(Mo–Au) deposit formation. *Econ. Geol.* **2003**, *98*, 1515–1533.
10. Zimmerman, A.; Stein, H.J.; Hannah, J.L.; Kozelj, D.; Bogdanov, K.; Berza, T. Tectonic configuration of the Apuseni–Banat–Timrok–Srednogorie belt, Balkans–South Carpathians, constrained by high precision Re–Os molybdenite ages. *Miner. Depos.* **2008**, *43*, 1–21.
11. Sutphin, D.; Hammarstrom, J.M.; Drew, L.J.; Large, D.E.; Berger, B.R.; Dicken, C.; DeMarr, M.W.; Billa, M.; Briskey, J.A.; Cassard, D.; *et al*. *Porphyry Copper Assessment of Europe, Exclusive of the Fennoscandian Shield*; U.S. Geological Survey: Reston, VA, USA, 2010.
12. Werle, J.I.; Ikramuddin, M.; Mutschler, F.E. Allard stock, La Plata Mountains, Colorado—An alkaline rock hosted porphyry copper precious metal deposit. *Can. J. Earth Sci.* **1984**, *21*, 630–641.

13. Mutschler, F.E.; Griffin, M.E.; Scott, S.D.; Shannon, S.S. Precious metal deposits related to alkaline rocks in the north American Cordillera—An interpretive review. *South Afr. J. Geol.* **1985**, *88*, 355–377.
14. Eliopoulos, D.G.; Economou-Eliopoulos, M. Platinum-group element and gold contents in the Skouries porphyry-copper deposit, Chalkidiki Peninsula, northern Greece. *Econ. Geol.* **1991**, *86*, 740–749.
15. Economou-Eliopoulos, M.; Eliopoulos, D.G. Palladium, platinum and gold concentrations in porphyry copper systems of Greece and their genetic significance. *Ore Geol. Rev.* **2000**, *16*, 59–70.
16. Eliopoulos, D.G.; Economou-Eliopoulos, M.; Strashimirov, S.; Kovachev, V.; Zhelyaskova-Panayotova, M. Gold, platinum and palladium content in porphyry Cu deposits from Bulgaria: A study in progress. *Geol. Soc. Greece* **1995**, *5*, 712–716.
17. Tarkian, M.; Stribrny, B. Platinum-group elements in porphyry copper deposits: A reconnaissance study. *Mineral. Petrol.* **1999**, *65*, 161–183.
18. Tarkian, M.; Hunken, U.; Tokmakchieva, M.; Bogdanov, K. Precious-metal distribution and fluid-inclusion petrography of the Elatsite porphyry copper deposit, Bulgaria. *Miner. Depos.* **2003**, *38*, 261–281.
19. Augé, T.; Petrunov, R.; Bailly, L. On the mineralization of the PGE mineralization in the Elastite porphyry Cu–Au deposit, Bulgaria: Comparison with the Baula-Nuasahi Complex, India, and other alkaline PGE-rich porphyries. *Can. Mineral.* **2005**, *43*, 1355–1372.
20. Piestrzynski, A.; Schmidt, S.; Franco, H. Pd-minerals in the Santo Tomas II porphyry copper deposit, Tuba Benguet, Philippines. *Miner. Pol.* **1994**, *25*, 12–31.
21. Tarkian, M.; Koopmann, G. Platinum-group minerals in the Santo Tomas II (Philex) porphyry copper–gold deposit, Luzon Island, Philippines. *Miner. Depos.* **1995**, *30*, 39–47.
22. Sheppard, S.M.F. Characterization and isotopic variations in natural waters. *Rev. Mineral. Geochem.* **1986**, *16*, 165–183.
23. Tobey, E.; Schneider, A.; Alegria, A.; Olcay, L.; Perantonis, G.; Quiroga, J. Skouries Porphyry Copper/Gold Deposit, Chalkidiki, Greece. In *Porphyry Hydrothermal Cu–Au Deposits*; Porter, T.M., Ed.; PGC Publishing: Adelaide, Australia, 1998; pp. 159–168.
24. Kockel, F.; Mollat, H.; Walther, H. *Erlanterungan zur Geologischen Karte der Chalkidiki und Angrenzender Gebiete*; Nord Griecheland: Hannover, Germany, 1977; scale 1:100,000. (in German)
25. Perantonis, G. Genesis of Porphyry Copper Deposits in Chalkidiki Peninsula and W. Thrace, Greece. Ph.D. Thesis, University of Athens, Athens, Greece, 17 June 1982.
26. Frei, R. Evolution of mineralizing fluid in the porphyry copper system of the Skouries deposit, Northern Chalkidiki (Greece): Evidence from combined Pb-Sr and stable isotope data. *Econ. Geol.* **1995**, *90*, 746–762.
27. Kroll, T.; Müller, D.; Seifert, T.; Herzig, P.M.; Schneider, A. Petrology and geochemistry of the shoshonite-hosted Skouries porphyry Cu–Au deposit, Chalkidiki, Greece. *Miner. Depos.* **2002**, *37*, 137–144.
28. Economou-Eliopoulos, M. Platinum-Group Element Potential of Porphyry Deposits. In *Mineralogical Association of Canada Short Course 35*; Mineralogical Association of Canada: Quebec, QC, Canada, 2005; pp. 203–245.

29. Naldrett, A.J. Secular variation of magmatic sulfide deposits and their source magmas. *Econ. Geol.* **2010**, *105*, 669–688.
30. Tarkian, M.; Eliopoulos, D.G.; Economou-Eliopoulos, M. Mineralogy of precious metals in the Skouries porphyry copper deposit northern Greece. *N. Jb. Miner. Mh.* **1991**, *12*, 529–537.
31. Taylor, H.P., Jr. Oxygen and Hydrogen Isotope Relationships in Hydrothermal Minerals Deposit. In *Geochemistry of Hydrothermal Ore Deposits*, 2nd ed.; Barnes, H.J., Ed.; John Wiley & Sons: Hoboken, NJ, USA, 1979; pp. 236–277.
32. Popov, P.; Popov, K. General Geologic and Metallogenic Features of the Panagyurishte Ore Region. In *Geology and Metallogeny of the Panagyurishte Ore Region (Srednogorie Zone, Bulgaria)*; Strashimirov, S., Popov, P., Eds.; ABCD-GEODE Workshop: Sofia, Bulgaria, 2000; pp. 1–7.
33. Strashimirov, S.; Bogdanov, K.; Popov, K.; Kehanov, R. Porphyry Systems of the Panagyurishte Ore Region. In *Cretaceous Porphyry-Epithermal Systems of the Srednogoric Zone, Bulgaria*; Bogdanov, K., Strashimirov, S., Eds.; Society of Economic Geologists: Littleton, CO, USA, 2003.
34. Strashimirov, S.; Petrunov, R.; Kanazirski, M. Mineral associations and evolution of hydrothermal systems in porphyry copper deposits from the Central Srednogorie zone (Bulgaria). *Miner. Depos.* **2002**, *37*, 587–598.
35. Bogdanov, K.; Filipov, A.; Kehayov, R. Au–Ag–Te–Se minerals in the Elatsite porphyry-copper deposit, Bulgaria. *Geochem. Mineral. Petrol.* **2005**, *43*, 13–19.
36. Von Quadt, A.; Peytcheva, I.; Kamenov, B.; Fanger, L.; Heinrich, C.A.; Frank, M. The Elatsite Porphyry Copper Deposit in the Panagyurishte Ore District, Srednogorie Zone, Bulgaria: U-Pb Zircon Geochronology and Isotope-Geochemical Investigations of Magmatism and Ore Genesis. In *The Timing and Location of Major Ore Deposits in an Evolving Orogen*; Geological Society Special Publication Volume 204; Blundell, D.J., Neubauer, F., von Quadt, A., Eds.; Geological Society of London: London, UK, 2002; pp. 119–135.
37. Kouzmanov, K. Genèse de la Concentration en Métaux de Base et Précieux de Radka et Elshitsa (Zone de Sredna Gora, Bulgarie): Une Approche Par l'étude Minéralogique, Isotopique et des Inclusions Fluids. Ph.D. Thesis, University of Orléans, Orléans, France, 12 May 2001. (in French)
38. Thompson, J.F.H.; Lang, J.R.; Stanley, C.R. Platinum Group Elements in Alkaline Porphyry Deposits, British Columbia. In *Geological Fieldwork 2001*; British Columbia Geological Survey: Victoria, BC, Canada, 2001; pp. 57–64.
39. Sotnikov, V.I.; Berzina, A.N.; Economou-Eliopoulos, M.; Eliopoulos, D.G. Palladium, platinum and gold distribution in porphyry Cu±Mo deposits of Russia and Mongolia. *Ore Geol. Rev.* **2001**, *18*, 95–111.
40. Li, C.; Naldrett, A.J. High chlorine alteration minerals and calcium-rich brines in fluid inclusions from the Strathcona Deep Copper Zone, Sudbury, Ontario. *Econ. Geol.* **1993**, *88*, 1780–1796.
41. Wood, S.A.; Mountain, B.W.; Pan, P. The aqueous geochemistry of platinum, palladium and gold: recent experimental constraints and a re-evaluation of theoretical predictions. *Can. Mineral.* **1992**, *30*, 955–982.
42. Wood, B.W. The Aqueous Geochemistry of the Platinum-Group Elements with Applications to Ore Deposits. In *Geology, Geochemistry, Mineralogy, Metallurgy and Beneficiation of Platinum-Group Elements*; Cabri, L.J., Ed.; Canadian Institute of Mining, Metallurgy and Petroleum: Montreal, QC, Canada, 2002; pp. 211–249.

43. Xiong, Y.; Wood, S.A. Experimental quantification of hydrothermal solubility of platinum-group elements with special reference to porphyry copper environments. *Mineral. Petrol.* **2000**, *68*, 1–28.
44. Hanley, J.J. The Aqueous Geochemistry of the Platinum-Group Elements (PGE) in Surficial, Low-T Hydrothermal and High-T Magmatic Hydrothermal Environments. In *Exploration for Platinum-Group Element Deposits*; Mungall, J.E., Ed.; Mineralogical Association of Canada: Quebec, QC, Canada, 2005; pp. 35–56.
45. Simon, A.C.; Pettke, T. Platinum solubility and partitioning in a felsic melt-vapor-brine assemblage. *Geochim. Cosmochim. Acta* **2009**, *73*, 438–454.
46. Barnes, S.J.; Liu, B. Pt and Pd mobility in hydrothermal fluids: Evidence from komatiites and from thermodynamic modelling. *Ore Geol. Rev.* **2012**, *44*, 49–58.
47. McInnes, B.I.A.; Cameron, E.M. Carbonated, alkaline hybridizing melts from a sub-arc environment: Mantle wedge samples from the Tabar-Lihir-Tanga-Feni arc, Papua New Guinea. *Earth Planet. Sci. Lett.* **1994**, *122*, 125–141.
48. Keith, J.D.; Christiansen, E.H.; Maughan, D.T.; Waite, K.A. The Role of Mafic Alkaline Magmas in Felsic Porphyry-Cu and Mo Systems. In *Mineralogical Association of Canada Short Course*; Mineralogical Association of Canada: Quebec, QC, Canada, 1998; pp. 211–243.
49. Moritz, R.; Kouzmanov, K.; Petrunov, R. Upper Cretaceous Cu–Au epithermal deposits of the Panagyurishte district, Srednogorie zone, Bulgaria. *Swiss Bull. Mineral. Petrol.* **2004**, *84*, 79–99.
50. Chambefort, I. The Cu–Au Chelopech Deposit, Panagyurishte District, Bulgaria: Volcanic Setting, Hydrothermal Evolution and Tectonic Overprint of a Late Cretaceous High-Sulfidation Epithermal Deposit. Ph.D. Thesis, University of Geneve, Geneve, Switzerland, 9 May 2005.
51. Kehayov, R.; Bogdanov, K.; Fanger, L.; von Quadt, A.; Pettke, T.; Heinrich, C. The Fluid Chemical Evolution of the Elatsite Porphyry Cu–Au–PGE Deposit, Bulgaria. In *Mineral Exploration and Sustainable Development*; Eliopoulos, D., Ed.; IOS Press: Amsterdam, The Netherlands, 2003; pp. 1173–1176.
52. Economou-Eliopoulos, M.; Eliopoulos, D.G. *Distribution of Rhenium (Re) in Molybdenites and Mo-Bearing Minerals of Greece and Its Economic Significance*; Athens University: Athens, Greece, 1996, pp. 1–30. (in Greek)
53. Berzina, A.N.; Sotnikov, V.I.; Economou-Eliopoulos, M.; Eliopoulos, D.G. Distribution of rhenium in molybdenite from porphyry Cu-Mo and Mo-Cu deposits of Russia (Siberia) and Mongolia. *Ore Geol. Rev.* **2005**, *26*, 91–113.
54. Voudouris, P.; Melfos, V.; Spry, P.G.; Bindi, L.; Moritz, R.; Ortelli, M.; Kartal, T. Extremely Re-rich molybdenite from porphyry Cu-Mo-Au prospects in northeastern Greece: Mode of occurrence, causes of enrichment, and implications for gold exploration. *Minerals* **2013**, *3*, 165–191.
55. Luck, J.M.; Allègre, C.J. The study of molybdenites through the ^{187}Re–^{187}Os chronometer. *Earth Planet. Sci. Lett*. **1982**, *61*, 291–296.
56. Meisel, T.; Walker, R.J.; Morgan, J.W. The osmium isotopic composition of the earth's primitive upper mantle. *Nature* **1996**, *383*, 517–520.
57. Mathur, R.; Marschik, R.; Ruiz, J.; Munizaga, F.; Leveille, R.A.; Martin, W. Age of mineralization of the Candelaria Fe oxide Cu–Au deposit and the origin of the Chilean iron belt, based on Re-Os isotopes. *Econ. Geol.* **2002**, *97*, 59–71.

58. Stein, H.J.; Markey, R.J.; Morgan, J.W.; Du, A.; Sun, Y. Highly precise and accurate Re–Os ages for molybdenite from the East Qinling molybdenum belt, Shaanxi Province, China. *Econ. Geol*. **1997**, *92*, 827–835.
59. Ripley, E.M.; Lambert, D.D.; Frick, L.R. Re-Os, Sm-Nd, and Pb isotopic constraints on mantle and crustal contributions to magmatic sulfide mineralization in the Duluth Complex. *Geochim. Cosmochim. Acta* **1998**, *62*, 3349–3365.
60. Lambert, D.D.; Foster, J.G.; Frick, L.R.; Hoatson, D.M.; Purvis, A.C. Application of the Re-Os isotopic system to the study of Precambrian sulfide deposits of Western Australia. *J. Earth Sci.* **1998**, *45*, 265–284.
61. Hart, G.L.; Johnson, C.M.; Shirey, S.B.; Clynne, M.A. Osmium isotope constraints on lower crustal recycling and pluton preservation at Lassen volcanic center, California. *Earth Planet. Sci. Lett.* **2002**, *199*, 269–285.
62. Mathur, R.; Ruiz, J.; Munizaga, F. Relationship between copper tonnage of Chilean base-metal porphyry deposits and Os isotope ratios. *Geology* **2000**, *28*, 555–558.
63. Mathur, R.; Ruiz, J.; Herb, P.; Hahn, L.; Burgath, K.P. Re–Os isotopes applied to the epithermal gold deposits near Bucaramanga, northeastern Colombia. *J. South Am. Earth Sci.* **2003**, *15*, 815–821.
64. Barra, F.; Ruiz, J.; Mathur, R.; Titley, S.; Schmitz, C.A. Re–Os study of sulfides from the Bagdad porphyry Cu-Mo deposit, northern Arizona, USA. *Miner. Depos*. **2003**, *38*, 585–596.
65. Janković, S.; Jelenković, R. Correlation between the Oraviţa-Krepoljin and the Bor-Srednjegorie metallogenic zones. *Rom. J. Miner. Depos.* **1997**, *78*, 57–70.
66. Karamata, S.; Kneević, V.; Pécskay, Z.; Djordjević, M. Magmatism and metallogeny of the Ridanj–Krepoljin Belt (eastern Serbia) and their correlation with northern and eastern Analogues. *Miner. Depos.* **1997**, *32*, 452–458.
67. Spry, P.G.; Mathur, R.D.; Bonsall, T.A.; Voudouris, P.; Melfos, V. Re–Os isotope evidence for mixed source components in carbonate-replacement Pb–Zn–Ag deposits in the Lavrion district, Attica, Greece. *Mineral. Petrol.* **2013**, *107*, doi:10.1007/s00710-013-0314-2.
68. Mungall, J.E.; Andrews, D.R.A.; Cabri, L.J.; Sylvester, P.J.; Tubrett, M. Partitioning of Cu, Ni, Au, and platinum-group elements between monosulfide solid solution and sulfide melt under controlled oxygen and sulphur fugacities. *Geochim. Cosmochim. Acta* **2005**, *69*, 4349–4360.
69. Sun, W.; Huang, R.; Liang, H.; Ling, M.; Li, C.; Ding, X.; Zhang, H.; Yang, X.; Ireland, T.; Fan, W. Magnetite–hematite, oxygen fugacity, adakite and porphyry copper deposits: Reply to Richards. *Geochim. Cosmochim. Acta* **2014**, *126*, 646–649.
70. Peach, C.L.; Mathez, E.A.; Keays, R.R. Sulphide melt-silicate melt distribution coefficients for the noble metals and other chalcophile metals as deduced from MORB: Implications for partial melting. *Geochim. Cosmochim. Acta* **1990**, *54*, 3379–3389.
71. Lefort, D.; Hanley, J.J.; Guillong, M. Sub-epithermal Au-Pd mineralization associated with an alkalic porphyry Cu–Au deposit, Mount Milligan, Quesnel Terrane, British Columbia, Canada. *Econ. Geol.* **2011**, *106*, 781–808.